DOE/ET-53088-361 IFSR #361

Suppression of Sawtooth Oscillations Due to Hot Electrons and Hot Ions

Y. Z. Zhang and *H. L. Berk*

Institute for Fusion Studies
The University of Texas at Austin
Austin, Texas 78712

January 1989

Suppression of Sawtooth Oscillations Due to Hot Electrons and Hot Ions

Y. Z. ZHANG and H. L. BERK
Institute for Fusion Studies
The University of Texas at Austin
Austin, Texas 78712

Abstract

The theory of $m = 1$ kink mode stabilization is discussed in the presence of either magnetically trapped hot electrons or hot ions. For stability hot ions require particles peaked inside the $q = 1$ surface, while hot electrons require that its pressure profile be increasing at the $q = 1$ surface. Experimentally observed sawtooth stabilization usually occurs with off-axis heating with ECRH and near axis heating with ICRH. Such heating may produce the magnetically trapped hot particle pressure profiles that are consistent with theory.

Recently in JET sawteeth have seen suppressed using ICRH on axis, producing the so-called monster sawtooth.[1,2] The mechanism of stabilization has been attributed to the presence of hot trapped ions[3] which produces a major modification to MHD theory. It is possible that hot electrons can play a similar stability role. In many of the tokamak experiments[4–9] with ECRH, partial sawtooth suppression is observed when the location of the resonance is well off-axis and the sawteeth are not suppressed with on-axis heating. Details of experimental investigation on this issue have been reported by DIII-D group.[4,5] They found that the sawtooth period and amplitude are very sensitive to the location of the ECH resonance in the plasma, with the largest sawtooth period and amplitude occurring when the resonance is near or just inside of the sawtooth temperature inversion surface, where the sawtooth period is extended by a factor of 4. Qualitatively the result fit models proposed by Park[10] and Westerhof[11] which require magnetic island formation to explain the sensitivity of the sawtooth stabilization to the location of resonance. However, no $m = 1$ island formation is observed in the ECRH experiments during the suppressed phase. It is also possible that a transport process associated with ECRH heating is responsible for sawtooth suppression, although a specific mechanism has not been identified.

In this letter we suggest a possible alternative sawtooth stabilization mechanism for ECRH which can arise if hot trapped electrons are created during heating. This stabilization mechanism has a different prediction than the stabilization mechanism with hot ions. We find that in order to suppress sawteeth with ICRH a hot trapped particle distribution is required peaked within the $q = 1$ surface. In contrast, for ECRH suppression requires hot electrons peaked off-axis with a rising gradient at the $q = 1$ surface.

To describe the internal kink stability use is made of the dispersion relation[3,12]

$$\omega_A \delta\hat{W} - i\sqrt{\omega\left(\omega - \omega_i^*\right)} = 0, \tag{1}$$

where ω_i^* is the ion diamagnetic frequency, ω_A is the Alfvén frequency, $\delta\hat{W} = \delta\hat{W}_c + \delta\hat{W}_h$. $\delta\hat{W}_c$ is the normalized MHD free energy of background plasma. We shall use the specific

$\delta\hat{W}_c$ obtained by Bussac[13]

$$\delta\hat{W}_c = 3\left(1-q(0)\right)\left(\frac{13}{144}-\tilde{\beta}_p^2\right)\left(\frac{r_s}{R}\right)^2 \tag{2}$$

with

$$\tilde{\beta}_p = -\left(\frac{8\pi}{B_p^2}\right)\int_0^{r_s/a} dx\, x^2\left(\frac{dP}{dx}\right), \tag{3}$$

where B_p is the poloidal field at the $q=1$ surface, P is the background plasma pressure, r_s is the position of the $q=1$ surface, a and R the minor and the major radius respectively, $q(0)$ the safety factor at $x \equiv r/a = 0$. $\delta\hat{W}_h$ is the frequency-dependent free energy contributed from hot particles. A somewhat simple but instructive model gives[14]

$$\delta\hat{W}_h = \tilde{\beta}_h\frac{\omega}{\bar{\omega}_{dh}}\ln\left(1-\frac{\bar{\omega}_{dh}}{\omega}\right) \tag{4}$$

with

$$\tilde{\beta}_h = -\left(\frac{R}{3a}\right)I\left(\kappa_0^2\right)a\frac{\partial\left\langle\beta_h\right\rangle}{\partial r}, \tag{5}$$

where $\langle\beta_h\rangle$ is the poloidally averaged toroidal beta value for the hot particles $I\left(\kappa_0^2\right) \equiv 2E\left(\kappa_0^2\right)/K\left(\kappa_0^2\right)-1$ ($\sim 1-\kappa_0^2$ for deeply trapped particles and for estimate we set $I\left(\kappa_0^2\right)\sim 1$), E and K are the complete elliptic integrals, $\kappa_0^2 = \kappa_0^2\left(\alpha_0\right)$ with $\kappa^2(\alpha) \equiv (R/2r)(1/\alpha-1+r/R)$, and $\bar{\omega}_{dh} \equiv (c/e_hBr_sR)\,I\left(\kappa_0^2\right)E_{\max}$ denotes the line average drift frequency of the trapped hot particles with $E_{\max}$ the maximum energy, evaluated at $\kappa^2=\kappa_0^2$, $r=r_s$. In the calculation of $\delta\hat{W}_h$ expressed by Eq. (4) we have assumed that $\partial\left\langle\beta_h\right\rangle/\partial r$ is a constant within the $q=1$ surface, and we have neglected an ω independent term of the order $(1-q(0))\left(\bar{\omega}_{dh}/\omega\right)\theta_r\sin\theta_r$, where θ_r is the typical poloidal angle width of the trapped particles. Thus this term can be neglected for sufficiently small $1-q(0)$ or θ_r.

Several analyses of the dispersion relation, Eq. (1), have been made for hot ions.[3,12,14–16] However, our study of the stabilizing effect due to hot electrons on the $m=1$ internal kink mode is new. In the absence of hot particles the MHD mode are determined by solving

$\omega_A \delta\hat{W}_c = i\sqrt{\omega\left(\omega - \omega_i^*\right)}$. The MHD mode is driven unstable by $\delta\hat{W}_c < 0$ for $\omega_i^* = 0$. The finite ω_i^* is found stabilizing to the MHD mode, with two marginally stable modes arising for $\omega_i^* > -2\omega_A \delta\hat{W}_c \left(\delta\hat{W}_c < 0\right)$,[12]

$$\omega = \frac{1}{2}\left(\omega_i^* \pm \sqrt{\omega_i^{*2} - 4\omega_A^2 \delta\hat{W}_c^2}\right). \tag{6}$$

This description is altered in the presence of hot particles. However, one obtains differing effects from hot ions and hot electrons. For hot ions, the drift frequency $\bar{\omega}_{dh}$ is in the same direction as the mode frequency ω, which gives rise to a wave-hot particle resonance, which contributes an imaginary part to $\delta\hat{W}_h$ even if ω is real [Eq. (4)]. The detailed analysis of the dispersion relation[16] only gives stabilization when the trapped hot ions are peaked inside the $q = 1$ surface. In contrast, the drift frequency of hot electrons is in the opposite directions of the mode frequency given by Eq. (6), so that $\delta\hat{W}_h$ of hot electrons is purely real for real ω. Thus hot electrons do not contribute a dissipative effect for the two modes of Eq. (6), and thus is not a source for a dissipative instability (e.g., with hot ions the slow fishbone mode found by Coppi and Porcelli[12] is due to hot ion inverse dissipation destabilizing the ω_i^* mode, which should not arise in an ECH heated plasma). Further, $\delta\hat{W}_h$ is positive (or negative) when $\partial\left\langle\beta_h\right\rangle/\partial r$ is positive (or negative). The positive $\delta\hat{W}_h$, provided by positive hot pressure gradient within the $q = 1$ surface, diminishes the driving force from negative $\delta\hat{W}_c$, and results in a stabilizing effect on the MHD mode. It should be emphasized that this stabilizing mechanism due to hot electrons is effective only if $\omega/\bar{\omega}_{dh} \gg (1 - q(0))\,\theta_r \sin\theta_r$, our condition for neglecting other hot electron terms.[17]

When the hot pressure gradient is positive the precessional mode is positive energy and not destabilized by dissipation. It can be seen from Eq. (4) that the pole contribution to $\delta\hat{W}_h$ is possible only if $\bar{\omega}_{dh}/\omega > 1$, and independent of sign of $\bar{\omega}_{dh}$. Therefore, a marginally stable precessional mode can be found only for positive $\tilde{\beta}_h$, or negative hot pressure gradient. We also point out that the precessional mode destabilized by the negative pressure gradient is in the opposite direction of ω_i^* for electrons and in the same direction as ω_i^* for ions. For

most parameter cases in the unstable region we find two unstable modes with hot electrons, and only one unstable mode with hot ions.

The stability boundaries are numerically obtained by solving the dispersion relation given by Eq. (1). In Fig. 1a and b the stability boundaries for electrons and ions, respectively, are shown in the $\hat{n}_h' - \hat{\omega}_i^*$ plane, where $\hat{n}_h' \equiv \tilde{\beta}_h \omega_A / |\bar{\omega}_{dh}| \sim \hat{s} \left\langle n_{h[12]} \right\rangle_\theta (r_s/L_{p_h}) R_{[m]} / \sqrt{n_{[13]}}$, and $\hat{\omega}_i^* \equiv \omega_i^* / |\bar{\omega}_{dh}| = (T_i/E_h)(R/L_{p_i})$, $\hat{s} \equiv r_s (dq/dr)_{r_s}$, the shear at r_s, L_{p_h} and L_{p_i} the scale length of the hot particle and background ion pressure gradient, respectively. $n_{h[12]}$ and $n_{[13]}$ the hot particle density in 10^{12}cm^{-3} and the background plasma density in 10^{13}cm^{-3} respectively, $R_{[m]}$ the major radius in meter. The stability boundary of $\delta\tilde{W}_c = -0.5$ in Fig. 1a corresponds to $\hat{n}_h' = 0.0$, implying the stabilization due to finite Larmor radius (FLR) of background ions. For $\delta\tilde{W}_c < -0.5$ the FLR effect is insufficient to achieve marginal stability. We also note that heating by itself, even without hot particles, extends the stability region due to increased FLR effects. In addition a positive hot electron pressure gradient provides a stabilizing force by diminishing the MHD free energy, to achieve marginal stability for $\delta\tilde{W}_c < -0.5$ at $\hat{n}_h' < 0$. With ions the stable region for negative $\delta\tilde{W}_c$ only exists for $\hat{n}_h' > 0$. In Fig. 1a (for hot electrons) the stable (or unstable) region is the area below (or above) one curve corresponding to a given value of $\delta\tilde{W}_c$. The more negative the $\hat{n}_h'$, the more stable the system. In addition there is a second marginal curve (given by the dashed lines), which corresponds to the threshold for the precessional mode (above the dashed line is instability). For almost all parameters the precessional mode lies in an unstable, and thus probably inaccessible region. However, in Fig. 1b (for hot ions) the stable region is restricted to the area enclosed by one curve corresponding to a given value of $\delta\tilde{W}_c$. For $\hat{\omega}_i^* > 0.5$ there is no stable region. The smaller the $\delta\tilde{W}_c$, the larger the stable region.

To help understand the stability diagram we schematically illustrate in Fig. 2a and b the locus of solution of the dispersion relation, Eq. (1), in the complex ω-plane under the influence of hot electrons and ions, respectively, for a given $\left|\delta\hat{W}_c\right| \omega_A < \omega_i^*/2$ with $\delta\hat{W}_c < 0$.

The arrows indicate the direction of increase of $\tilde{\beta}_h$. The dots in the figure denote the ω value when $\tilde{\beta}_h = 0$ (a_1, a_2, a_3 in Fig. 2a, and b_1, b_2 in Fig. 2b). At points of a_1, a_2 and b_1, b_2 the real frequencies are determined by Eq. (6). It can be seen from Fig. 2 that the behavior of the frequency as $\tilde{\beta}_h$ varies is quite different for hot ions and hot electrons. For hot ions there is always one unstable mode as $\tilde{\beta}_h$ approaches zero. The low-frequency mode is destabilized by negative $\tilde{\beta}_h$, while high-frequency mode (ω_i^* mode) is destabilized by positive $\tilde{\beta}_h$. The further increase of $\tilde{\beta}_h$ stabilizes the ω_i^* mode. At yet higher $\tilde{\beta}_h$ the stable mode is converted to the precessional instability. Thus, for moderate value of $\tilde{\beta}_h$ we see the stability band that exists in Fig. 1b. Notice that for a given $\tilde{\beta}_h$ only one possible unstable mode can arise. In contrast to ion case, when hot electron $\tilde{\beta}_h$ crosses zero, the two real mode (near a_1 and a_2) still remain real until $\tilde{\beta}_h$ increases up to a certain positive value, where two complex conjugate modes emerge (denoted by a^* in Fig. 2a). This is the $\tilde{\beta}_h$-value that is calculated in the marginal stability boundary of Fig. 1a. When the $\tilde{\beta}_h$ goes to negative value, these two real modes remain two real ones until $\tilde{\beta}_h = \delta\tilde{W}_c/\left[\hat{\omega}_i^* \ln\left(1 + 1/\hat{\omega}_i^*\right)\right]$, where the high-frequency mode (ω_i^* mode) terminates at the branch point $\omega = \omega_i^*$, and only the low-frequency mode persists for more negative $\tilde{\beta}_h$. On the other hand, the separate precessional mode is destabilized by positive $\tilde{\beta}_h$ as indicated by curves a and b in Fig. 1a. Its locus is shown in Fig. 2a by the curve with the dot of a_3 on it. Thus, for sufficiently high positive $\tilde{\beta}_h$ of hot electron ($\tilde{\beta}_h$ goes beyond both the points of a^+ and a^* in Fig. 2a) there exist two distinct unstable modes.

If for hot electrons $\left|\delta\hat{W}_c\right| \omega_A > \omega_i^*/2 \left(\delta\hat{W}_c < 0\right)$ the system is unstable if $\tilde{\beta}_h = 0$. This mode is stabilized as $\tilde{\beta}_h$ goes negative at an appropriate value that can be found from Fig. 1a. As one goes to positive $\tilde{\beta}_h$ the unstable mode persists, but a second unstable mode arises when the critical $\tilde{\beta}_h$ for the precessional mode is reached.

Now, we try to relate the above theoretical prediction with experimental parameters for sawtooth suppression in DIII-D and JET.

The operating parameters are available[4] in DIII-D with second harmonic ECRH using

the X-mode outside launch system up to power of 0.85 MW. In this case the sawtooth period was greater than the 80 msec length of the rf pulse when the ECH resonance was placed near the sawtooth inversion surface ($r_s \sim 20$ cm) and the density at r_s is about $1.2 \times 10^{13}\text{cm}^{-3}$, $B \sim 1$ Tesla, $T_i \sim 1$ kev, $L_{p_i} \sim 30$ cm, $R \sim 170$ cm the shear $\hat{s}$ is estimated 0.5–1.0 (we take $\hat{s} \sim 0.75$ in the following estimate). However, the sawtooth period changed from 80 to 25 msec when the heating was shifted 3 cm from the sawtooth inversion toward either the center or the edge of the plasma. According to the above theory, this fact implies that the FLR stabilization above is insufficient to have the sawtooth suppression, i.e., $\delta\tilde{W}_c < -0.5$. Using the above parameters in DIII-D, we estimate $\omega_i^*/\omega_A \sim 6 \times 10^{-3}$. Thus the magnitude of MHD energy drive $\left|\delta\hat{W}_c\right|$ should be greater than 3×10^{-3}. Note that using the Bussac formula (Eq. (2)) and assuming $q(0) = 0.75$, $\delta\hat{W}_c \sim 0.001\left(1 - 11\tilde{\beta}_p^2\right)$, $\tilde{\beta}_p > 0.6$ is then required to overcome FLR stabilization without any hot particles. When the MHD free energy is doubled from this value, i.e., $\delta\tilde{W}_c = -1.0$, the sawtooth stabilization requires $\hat{n}_h' \sim -0.4$ (Fig. 1a), if we take $E_h \sim 20$ kev. The required hot trapped electron density is found to be $4 \times (L_{p_h}/r_s) \times 10^{11}\text{cm}^{-3}$. If we take $L_{p_h} \sim 3$ cm, (such a small scale length is suggested by experiment because of the sensitivity of the change of sawtooth period with the ECRH resonance position) then about 1% of hot trapped to background electron density around the $q = 1$ surface is capable of gaining sawtooth stabilization for the doubled MHD free energy. This amount of hot trapped electrons is a reasonable expectation. Our theory offers a mechanism of stabilization that is quite sensitive to heating on the $q = 1$ surface. However, more detailed investigations should be performed to confirm this explanation and it is especially important to verify that a hot trapped electron component is created.

The ICRH switch-off experiment in JET[2] suggests that the loss of fast ions are the dominant destabilizing effect while the FLR stabilization is insufficient to sustain the monster sawtooth after the fast ions are lost. We then infer that the magnitude of the $\delta\tilde{W}_c = \delta\hat{W}_c(\omega_A/\omega_i^*)$ should be greater than 0.5 during the monster sawtooth period of the ICRH

switch-off experiment. Making use of the following estimates $T_i \sim 4\,\mathrm{kev}$, $E_h \sim 500\,\mathrm{kev}$, $L_{p_i} \sim 1.2\,\mathrm{m}$, $R \sim 3\,\mathrm{m}$, we find $\hat{\omega}_i^* \sim 0.02$. Thus the stabilization requires a range of $\hat{n}_h'$ to be $0.1 \lesssim \hat{n}_h' \lesssim 0.3$, as seen from Fig. 1b. Then, the hot trapped ion density should be within the range of (0.5–1.5) $(L_{p_h}/r_s\hat{s}) \times 10^{11}\mathrm{cm}^{-3}$ for obtaining the stabilization. This rough estimate for the hot trapped ion density is consistent with present experimental estimates.[18] We note that the stable window disappears for higher $\left|\delta\tilde{W}_c\right|$ value, for example, the stable window vanishes for $\delta\tilde{W}_c = -2.5$ at $\hat{\omega}_i^* = 0.02$. Thus, this example illustrates that the hot particle contribution produces a considerable expansion (a factor of 5) of the stabilization window over a solely FLR stabilization mechanism. Stabilization with ICRH should be less sensitive to the resonance heating position than with ECRH, although heating needs to be confined to within the $q = 1$ surface.

Acknowledgments

We would like to acknowledge A. Wootton, who suggested the investigation of hot electron effects on sawtooth oscillations. We are also grateful for helpful discussions with R. T. Snider, M. S. Chu, and V. Chan of the DIII-D Group and the encouragement of Dr. D. Baldwin. This work was supported by U. S. Dept. of Energy Contract No. DE-FG05-80ET-53088.

References

1. D. Campbell, et al., Phys. Rev. Lett. **60**, 2148 (1988).

2. D. Campbell, et al., 15th European Physical Society Conference on Controlled Fusion and Plasma Heating, Dubrounik, 1988.

3. B. Coppi, R. J. Hastie, S. Migliuolo, F. Pegararo, and F. Porcelli, Phys. Lett. **A132**, 267 (1988).

4. DIII-D Group, 12th International Conference on Plasma Physics and Controlled Nuclear Fusion Research (Nice, France), IAEA-CN-50/E-I-2 (1988).

5. R. T. Snider, D. Content, R. James, J. Lohr, M. Mahdavi, R. Prater, and B. Stallard, Phys. Fluids **B1**, 404 (1989).

6. PDX Group, Proceedings in Heating in Toroidal Plasmas, Rome, 1984 (International School of Plasma Physics, Varenna, 1984), Vol. II, p. 809.

7. R. M. Sillen, H. W. Pickaar, T. Oyevaar, E. P. Gozbunov, A. A. Bagdasorov, and N. L. Vasom, Nucl. Fusion **26**, 303 (1986).

8. CLEO Group, Proceedings in Heating in Toroidal Plasmas, Rome, 1984 (International School of Plasma Physics, Varenna, 1984), Vol. II, p. 795.

9. TFR Group, FOM ECRH Team, in **Controlled Fusion and Plasma Heating**, Schliersee, 1986 (European Physical Society, 1986) Vol. II, p. 207.

10. W. Park, D. A. Monticello, and T. K. Chu, Phys. Fluids **30**, 285 (1987).

11. E. Westerhof and W. J. Goedheer, in **Controlled Fusion and Plasma Heating**, 14–18 April 1986, Schliersee 1986 (European Physical Society, 1986) Vol. I, p. 132.

12. B. Coppi and F. Porcelli, Phys. Rev. Lett. **57**, 2272 (1986).

13. M. N. Bussac, R. Pellat, D. Edery, and J. L. Soulé, Phys. Rev. Lett. **35**, 1638 (1975).

14. L. Chen, R. B. White, and M. N. Rosenbluth, Phys. Rev. Lett. **52**, 1122 (1984).

15. R. B. White, M. N. Bussac, and F. Romanelli, Princeton Plasma Physics Laboratory Report PPPL-2540 (1988).

16. Y. Z. Zhang, H. L. Berk, and S. M. Mahajan, Nucl. Fusion **29**, 847 (1989).

17. F. Pegoraro and F. Porcelli, Private Communication.

18. T. Hellston, et al., Bull. Am. Phys. Soc. **33**, 2031 (1988).

Figure Captions

1. Stability boundaries in $\hat{n}'_h - \hat{\omega}^*_i$ plane for various values of $\delta\tilde{W}_c \equiv \delta\hat{W}_c\omega_A/\omega^*_i$.

   (a) The stability boundaries for hot electrons. Solid curves are boundaries determined by the MHD mode for $\delta\tilde{W}_c = -0.1, -0.25, -0.5, -0.75, -1.0, -1.5, -2.0$. The dashed curves are boundaries determined by the precessional mode for $\delta\tilde{W}_c = -1.0$ (curve a), -0.01 (curve b). The stable region is the area below the curve corresponding to a given $\delta\tilde{W}_c$.

   (b) The stability boundaries for hot ions for $\delta\tilde{W}_c = 0.0, -0.01, -0.05, -0.1, -0.25, -0.5, -1.0, -2.5$. The stable region is the area enclosed by the boundary corresponding to a given value of $\delta\tilde{W}_c$.

2. The schematical illustration of locus of solution of the dispersion relation Eq. (1) in the complex ω-plane under the influence of hot particles. The arrows indicate the direction of increase of $\tilde{\beta}_h$.

   (a) For hot electrons $\tilde{\beta}_h = 0$ at a_1, a_2, a_3. a^* and a^+ denote the points of marginal stability in Fig. 1a for MHD mode and precessional mode, respectively.

   (b) For hot ions $\tilde{\beta}_h = 0$ at b_1, b_2.

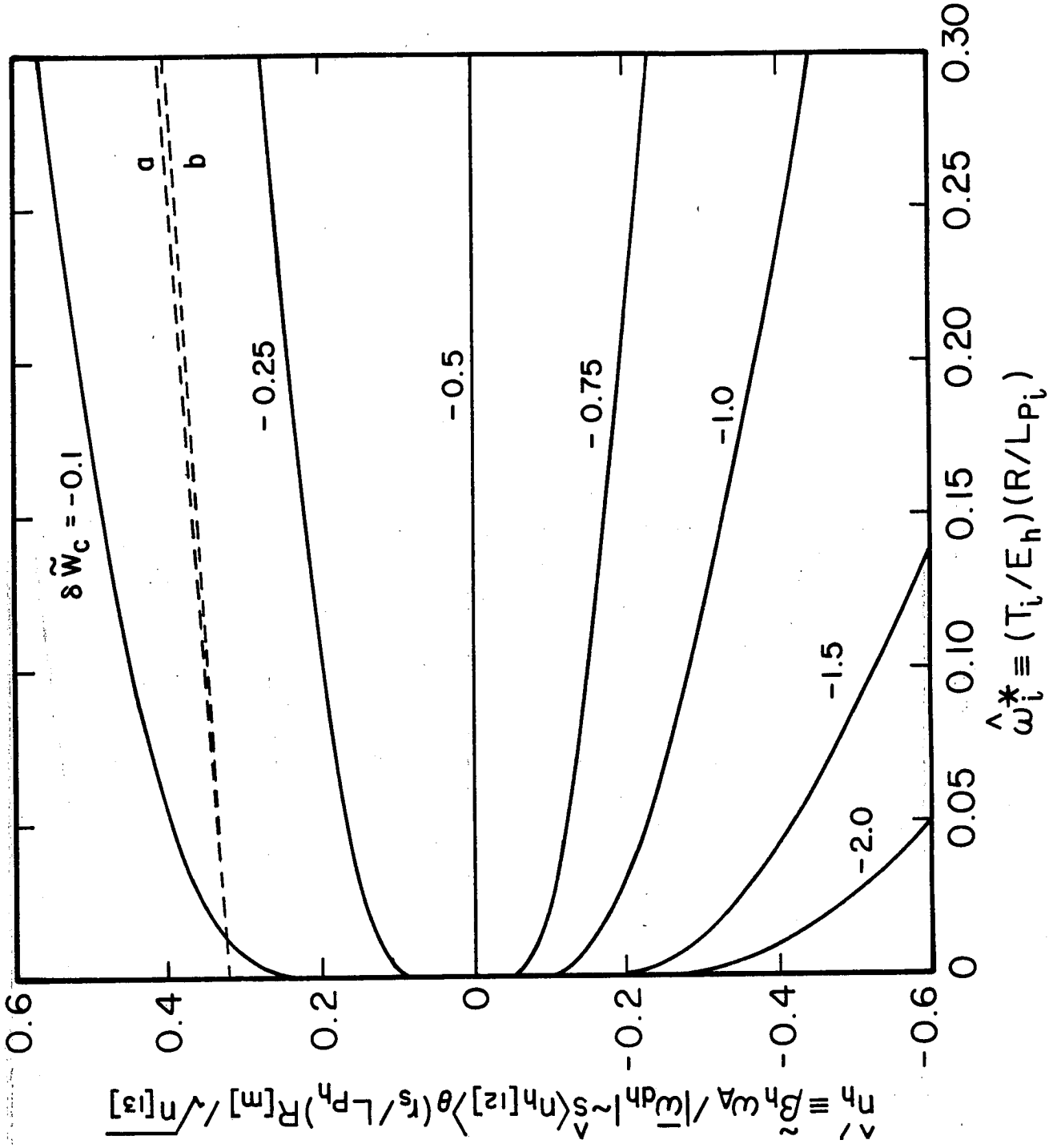
$\hat{\eta}_h' \equiv \beta_h^2 \omega_A / |\bar{\omega}_{dh}| \sim \hat{s} \langle n_h[12] \rangle \theta (r_s / L_{P_h}) R[m] / \sqrt{n[13]}$
$\hat{\omega}_i^* \equiv (T_i / E_h)(R / L_{P_i})$
$\delta \tilde{W}_c = -0.1$
-0.25
-0.5
-0.75
-1.0
-1.5
-2.0
a
b
0.6
0.4
0.2
0
-0.2
-0.4
-0.6
0
0.05
0.10
0.15
0.20
0.25
0.30

Figure 1a

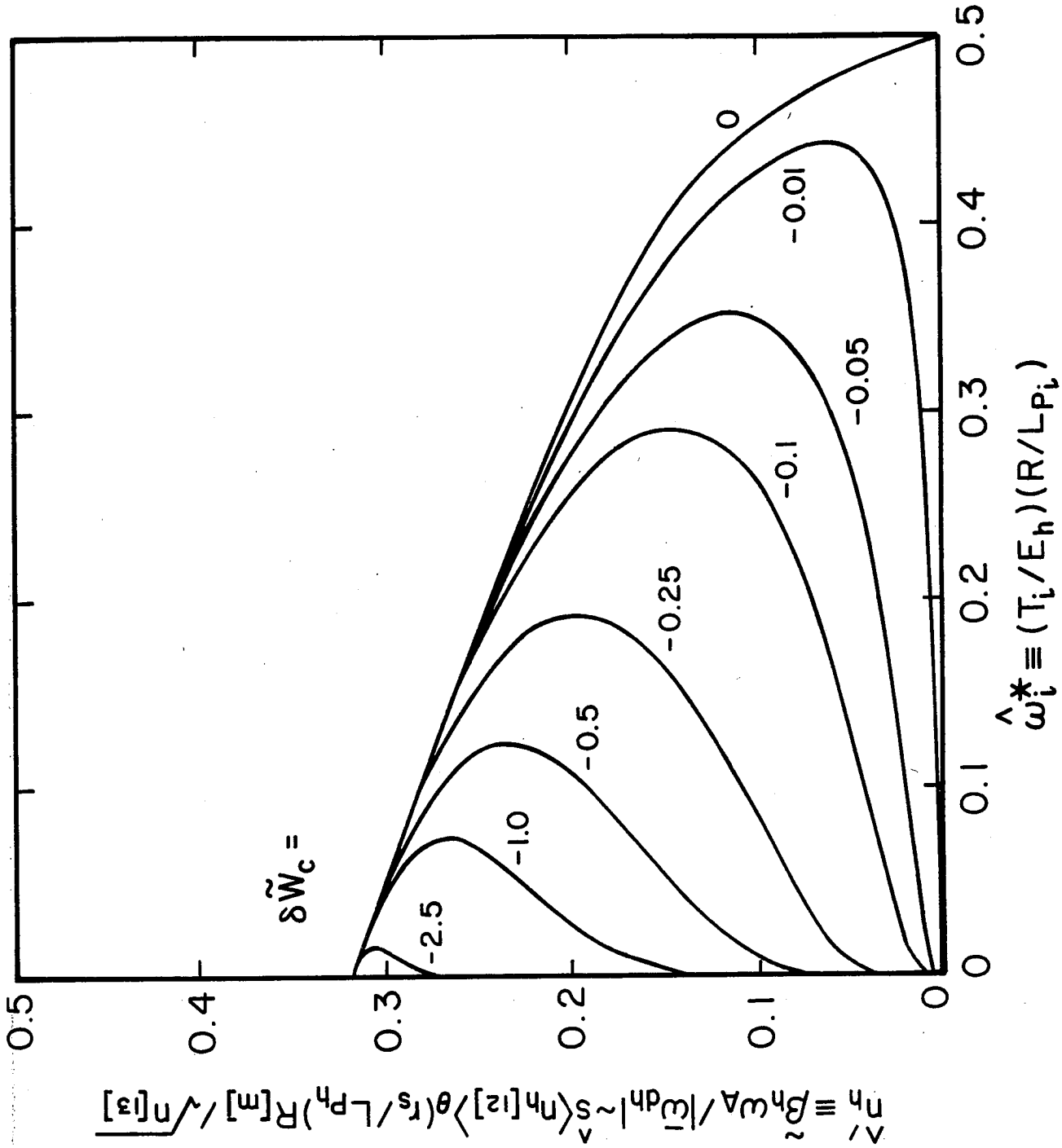
$\hat{n}_h' \equiv \tilde{\beta}_h \omega_A / |\bar{\omega}_{dh}| \sim \hat{s} \langle n_h[12] \rangle \theta(r_s/L_{P_h}) R[m] / \sqrt{n[13]}$
0.5
0.4
0.3
0.2
0.1
0
$\delta \tilde{W}_c =$
-2.5
-1.0
-0.5
-0.25
-0.1
-0.05
-0.01
0
0
0.1
0.2
0.3
0.4
0.5
$\hat{\omega}_i^* \equiv (T_i/E_h)(R/L_{P_i})$

Figure 1b

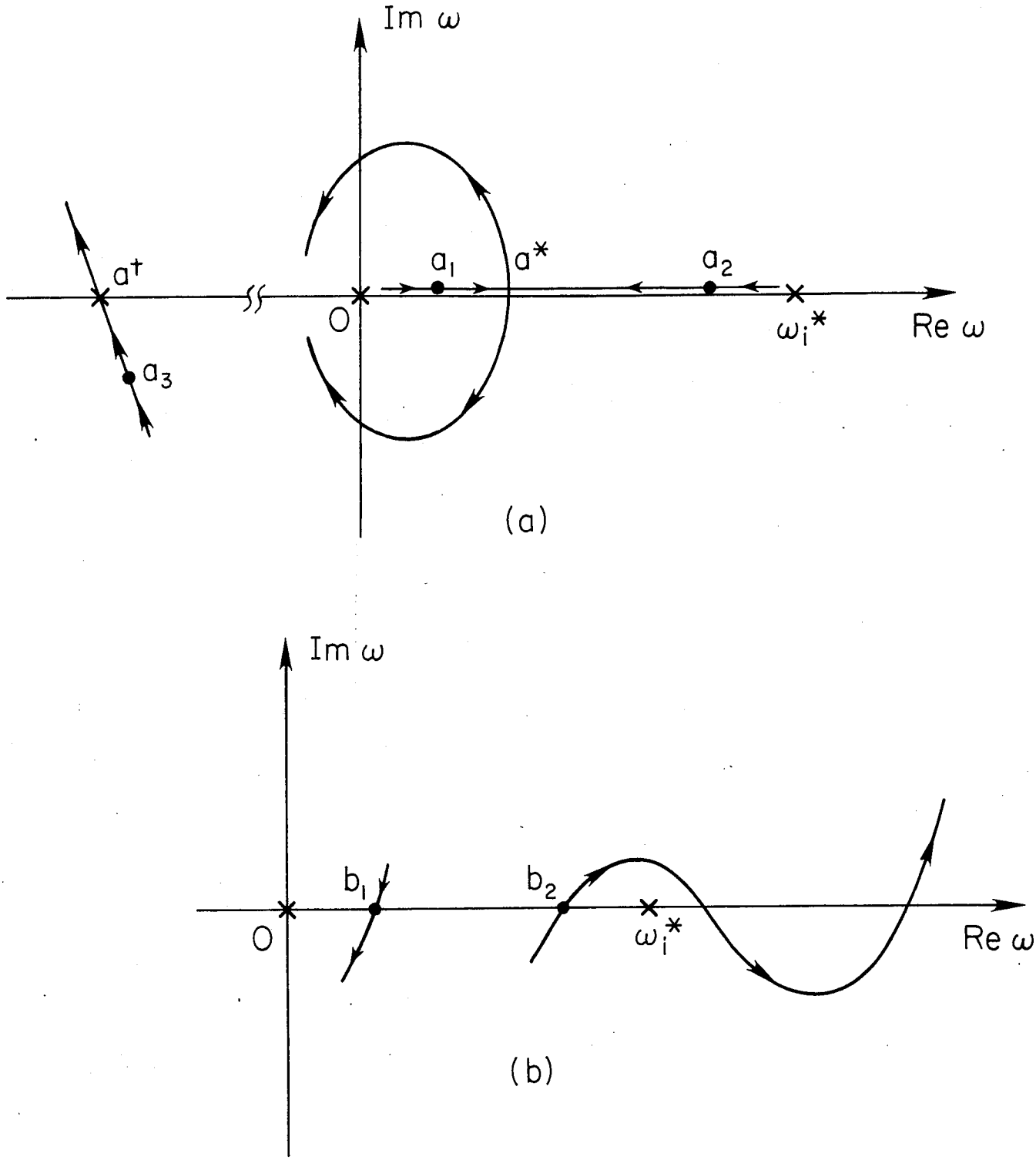

Figure 2